SYNTHESIS AND CHARACTERIZATION OF Fe(II), Mn(II), Co(II), Ni(II), Pd(II), Cu(II), Zn(II), Hg(II) AND Cd(II) COMPLEXES WITH HYDROXYBENZALDEHYDE DERIVATIVE OF DIACETYLMONOXIMEHYDRAZIDE

Dr. Sharad Sankhe[1*], Mr. Farhan Moosa[2]

Abstract

The synthesis of a novel ligand and its metal complexes. The hydroxybenzaldehyde derivative of diacetylmonoximehydrazide (HDMH*m*HB) ligand was prepared by reacting 3-hydroxybenzaldehyde with diacetylmonoxime hydrazide. Mononuclear complexes of this ligand of the type [M(DMH*m*HB)$_2$] were synthesised in the presence of MeOH, where M= Fe^{II}, Mn^{II}, Co^{II}, Ni^{II}, Pd^{II}, Cu^{II}, Zn^{II}, Hg^{II}, and Cd^{II}, and the metal: ligand molar ratio is (1:2). For Fe^{II}, Mn^{II}, Co^{II}, Ni^{II}, and Cu^{II} complexes, it is proposed that the metal ion complexes [[M(DMH*m*HB)$_2$] be six-coordinated with an N_4O_2 donor environment, and four-coordinated with an N_4 donor environment. The coordination of the ligand is performed by the oxime nitrogen, imine nitrogen, and phenolic oxygen atoms. Based on ^{1}H-NMR, ESR, FT(IR), elemental analysis (C, H, N), magnetic susceptibility tests, and electronic spectroscopy, the structures of the complexes were hypothesised.

Keywords: Hydroxybenzaldehyde, Schiff base, diacetylmonoxime, hydrazide compounds, metal complexes.

[1*]Professor, Department of Chemistry, Patkar-Varde College, Goregaon West, Mumbai-62, India.
[2]PhD scholar, Department of Chemistry, Patkar-Varde College, Goregaon West, Mumbai-62, India.

***Corresponding Author:** Dr. Sharad Sankhe
*Professor, Department of Chemistry, Patkar-Varde College, Goregaon West, Mumbai-62, India.

DOI: 10.48047/ecb/2023.12.si5a.0400

1. INTRODUCTION:

The coordination chemistry of oxime hydrazones[1-3] is quite interesting because it combines donor sites such as protonated/deprotonated oximino oxygen, an imine nitrogen of the hydrazone moiety, and an additional donor site (usually N or O) provided by the Schiff base[4-5]. The considerable research on structural studies of oxime complexes reveals some remarkable aspects of their coordination behaviour[6]. It may coordinate with one metal ion via the nitrogen atom and another via the oxygen atom[7]. As a result, it can form a proximate-bridged extended network[8]. The oxime-OH group's hydrogen atom can form potentially strong intra- or intermolecular hydrogen bonds with other donor atoms or groups[9-10]. Metal complexes containing non-deprotonated oximes can thus be considered supramolecular synthons capable of forming extended supramolecular networks via intermolecular hydrogen bonds. The orientation of the oxime group in these molecules impacts the dimensionality of the extended network significantly[11].

The coordination chemistry of trivalent oxime-hydrazones has been extensively studied due to biological activities[12-15]. To investigate the supramolecule-forming abilities of these Schiff bases, we synthesised two Schiff bases of diacetylmonoximehydrazide with m-hydroxybenzaldehyde. With this in mind, authors present the synthesis, characterisation, and spectroscopic studies of some metal (II) complexes of the type [M(DMH*m*HB)$_2$] obtained from the reaction of substituted hydroxybenzaldehyde derivative of diacetylmonoximehydrazide with metal (II) ions.

2. EXPERIMENTAL

2.1. Materials and Physical Measurements

Loba Chemical Co. (India) supplied all chemicals used without further purification. TMS was the internal standard for ^{1}H-NMR spectra recorded on a Bruker 400 MHz spectrometer in DMSO-d_6. FT(IR) spectra were recorded using a Bruker-ALPHA infrared spectrometer with Fourier transform (FTIR-4100). The Eurovetor-CA-3000 was used to measure the C, H, and N analyser (India). A Gouy balance measured magnetic susceptibility at room temperature (27^{o}C). UV-visible spectra were measured in the regions using a JASCO V-650 Spectrophotometer (900–200 nm).

2.2. Synthesis of diacetylmonoximehydrazide:

For 1 hour, a methanolic solution of diacetylmonoxime (10.1 g, 0.10 mol) was mixed with an excess of hydrazine hydrate, $NH_2NH_2.H_2O$ (6.25 ml, 0.125 mol) (80%, d = 1.03). After 1 hour of standing, the compound precipitated and was filtered and washed with distilled water. Recrystallisation from ethanol yielded pure diacetylmonoximehydrazide.

2.3. Synthesis of Schiff base HDMH*m*HB ligand:

A 50-ml methanol solution of diacetylmonoximehydrazide (11.50 g, 0.10 mol) was added to a 50-ml methanol solution of 3-hydroxybenzaldehyde (13.42 g, 0.11 mol), and the reaction mixture was stirred with refluxing for 3 hours. The resulting solid was filtered and thoroughly washed with water (2 x15 ml) before being washed with diethyl ether (2 x5 ml). **Scheme-1** shows how the solid was recrystallised from methanol.

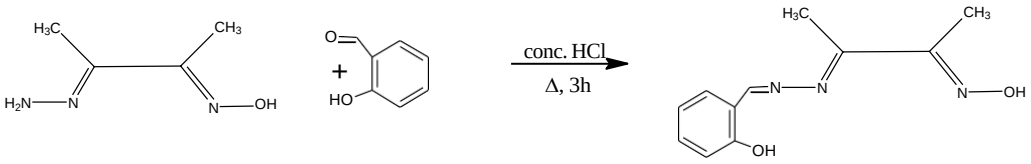

Scheme-1: Preparation of HDMH*m*HB ligand

2.4. Synthesis of the complexes:

All complexes were prepared the same way, by reacting a methanolic solution of the ligand with an aqueous solution of metal salts in a 2:1 molar ratio. One of the complex preparations is described in the;

The colour of the solution changed immediately when metal salts ($FeSO_4$, $MnCl_2$, $CoCl_2$, $NiCl_2$, $PdCl_2$, $CuCl_2$, $ZnCl_2$, $CdCl_2$ and $HgCl_2$) (each 0.5 mmol) were added to a 25 ml methanolic solution of the ligand (2.19g, 1mmol). The volume of the solution was diluted to 20 mL and filtered after 5 hours of stirring. The resulting material was cleaned with methanol (3x3 ml) and diethyl ether (2x5 ml), as shown in **Scheme-2**. The results of the compositional and spectroscopic data are shown in **Table-1**.

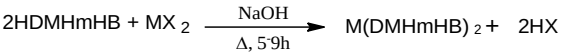

Where M = Fe^{II}, Mn^{II}, Co^{II}, Ni^{II}, Pd^{II}, Cu^{II}, Zn^{II}, Hg^{II}, and Cd^{II}, X = Cl, SO_4

Scheme-2: Preparation of metal complexes

Antimicrobial Assay

Antibacterial Activity

The National Centre for Medical Research (NCMR) Microbial Culture Collection (MCC) in Pune provided all bacterial strains. Antimicrobial experiments used Muller Hilton agar media autoclaved at 10 lbs/in^2 for 15 minutes. Each microbial strain was cultured by swabbing 20 mL of Muller Hilton agar medium into a Petri dish and waiting 15 minutes for the medium to absorb the culture. The wells (6 mm in diameter) were drilled using a sterile borer, and 100 L solutions of each chemical, reconstituted in DMSO, were introduced to the pre-inoculated plates. For 24 hours, the containers were kept at 37 °C. Each chemical's antibacterial activity was calculated using the wells' zone of inhibition. The positive control was streptomycin, and the negative control was DMSO. For each organism, the technique was repeated three times in separate plates.

Antifungal Activity

Aspergillus fumigatus and Aspergillus flavus were used to test the chemicals in the cup-plate method. After pipetting the test solution into 5-mm-diameter, 1-mm-thick discs, plates were incubated at 37 °C for 72 hours. The injected fungi grew as the test solution diffused. 36 hours of 37 °C incubation, they assessed the inhibition's diameter. Compounds with good antifungal activity underwent minimum inhibitory concentration tests. During overnight incubation, an antifungal compound's MIC suppressed observable microorganism growth. MIC was used in diagnostic laboratories to test new antimicrobial drugs and microorganism resistance.

3. RESULTS AND DISCUSSION:

According to the analytical results, the complexes displayed stoichiometry of type ML_2, where M stands for nickel, cobalt, copper, and mercury, and L stands for Schiff base ligand (**Table-1**). All complexes had colour, were non-hygroscopic, stable at room temperature, and broke down when heated. The complexes were insoluble in common organic solvents as well as in water. The complexes' non-electrolytic character is indicated by the low measured molar conductance values (0.85-1.80 Ω^{-1} cm^2 mole^{-1}). These values rule out any dissociation of the complexes in nitrobenzene[15-16].

Table-1: Physical and Analytical data of HDMH*m*HB ligand and its transition Metal (II) complexes

Compound	Colour	% Yield	MP/DP in ^oC	% Element Content, Expected (Observed)					Molar Cond	Magnetic Moments
				C	**H**	**N**	**O**	**M**		
HDMH*m*HB	Yellow	66.47	201	60.26 (60.23)	5.98 (5.97)	19.17 (19.15)	14.60 (14.58)	-	-	-
[Fe(DMH*m*HB)$_2$]	Blue	84.55	273	53.68 (53.39)	4.88 (4.87)	17.08 (17.01)	13.00 (12.94)	11.40 (11.39)	1.47	Dia
[Co(DMH*m*HB)$_2$]	Brown	77.59	261	53.33 (52.96)	4.85 (4.77)	16.97 (16.83)	12.90 (12.78)	11.90 (11.32)	1.13	3.60
[Ni(DMH*m*HB)$_2$]	Green	81.31	269	53.37 (53.18)	4.85 (4.80)	16.98 (16.88)	12.90 (12.39)	11.90 (11.69)	0.74	1.65
[Pd(DMH*m*HB)$_2$]	Brown	86.14	263	48.71 (48.63)	4.43 (4.42)	15.50 (15.41)	11.80 (11.78)	19.56 (19.37)	0.68	Dia
[Cu(DMH*m*HB)$_2$]	Green	79.21	247	52.85 (52.29)	4.80 (4.79)	16.82 (16.71)	12.80 (12.73)	12.70 (12.69)	0.85	9.76
[Mn(DMH*m*HB)$_2$]	Brown	74.49	266	53.88 (53.59)	4.89 (4.73)	17.11 (16.98)	13.04 (12.70)	11.19 (10.89)	1.19	10.58
[Zn(DMH*m*HB)$_2$]	Yellow	78.99	269	52.65 (52.59)	4.79 (4.73)	16.75 (16.68)	12.80 (11.70)	13.00 (12.87)	0.92	10.58
[Cd(DMH*m*HB)$_2$]	Yellow	77.70	267	48.14 (48.09)	4.38 (4.36)	15.32 (15.30)	11.70 (11.68)	20.50 (19.98)	1.22	10.58
[Hg(DMH*m*HB)$_2$]	Brown	76.41	281	41.51 (41.49)	3.77 (3.73)	13.21 (13.18)	10.06 (9.70)	31.54 (30.87)	0.77	10.58

3.1. FT(IR) Spectral Studies:

Table-2 exhibits FT(IR) spectrum data for the produced ligand and its complexes with Fe^{II}, Mn^{II}, Co^{II}, Ni^{II}, Pd^{II}, Cu^{II}, Zn^{II}, Hg^{II}, and Cd^{II} metal ions. The free HDMH*m*HB ligand FT(IR) spectrum showed a 3374 cm^{-1} band attributed to phenolic -OH. This band shifted to the lower side throughout the complexes, demonstrating that the phenolic OH group is involved in bonding[17-18]. A noticeable band is found at 3316cm^{-1}, attributed to the title ligand's oximino -OH. It was clear from the absence of this band in all the complexes that the hydroxyl group had deprotonated during complexation[19]. The prominent band at 1617 cm^{-1} seen in the free ligand was caused by the azomethine group's >C=NN- stretch[20]. This band shifted to the side with a lower wavenumber in all the complexes, indicating that the azomethine oxygen formed

bonds with metal ions[21]. The ν(C=NO) stretch of the oximino group was identified as the origin of a medium-to-strong intensity band at 1571 cm^{-1} in the free ligand[22]. It is predicted that the electron density in the azomethine link would decrease, and the >C=N- stretching absorption frequency would decrease due to the coordination of the Schiff base to the metal ions through the nitrogen atom[23]. This band, which has shifted to the lower wavenumber side in all complexes, suggests the involvement of oximino nitrogen in coordination with metal ions[24].

Studies are helpful because they provide direct knowledge about the coordination connection between the metal and ligand, even though the assignments of bands in the far-infrared region have been contentious throughout the years[25-26]. The stretching frequencies of the ν(M-O) and ν(M-N) bonds, respectively, are responsible for the new weak intensity nonligand bands found in the complex's spectra in 523-560 cm^{-1} and 428-460 cm^{-1}.

Table-2: FT (IR) spectral bands of the ligand (HDMH*m*HB) and its transition metal (II) complexes (cm^{-1}):

Assignments	HDMHmHB	Fe(II)	Co(II)	Ni(III)	Pd(II)	Cu(II)	Mn(II)	Zn(II)	Cd(II)	Hg(II)
Oximino -OH	3316	-	-	-	-	-				-
Phenolic -OH	3173	3142	3148	3243	3171	3139	3142	3175	3174	3176
νC=C Ar.	3022	3010	3012	3005	3008	3025	3022	3021	3018	3021
νC=NN	1617	1590	1591	1588	1593	1590	1588	1591	1590	1598
νC=NO	1571	1539	1539	1547	1545	1546	1544	1549	1541	1540
νN-N	970	1002	1001	1003	1002	1007	1009	1009	1007	1003
νN→O	-	1202	1199	1206	1205	1205	1200	1997	1201	1206
νM-N	-	560	555	556	523	555	550	549	559	552
νM→N	-	429	482	451	460	452	430	435	458	444

3.2. Electronic absorption spectra:

The electronic absorption spectra of all prepared metal complexes were measured at room temperature in freshly prepared chloroform solution (10^{-2} to 10^{-4} M). **Tables-3** exhibit the spectral data and ligand field parameters.

The Fe (II) complex's electronic spectra revealed an absorption band at 905 nm typical of the $^5T_{2g}$ to ^5E_g transition in an octahedral environment[27]. Bands 678 and 608nm might be seen in the Co (II) complex's electronic spectrum. In an octahedral environment, these two bands can be attributed to the $^4T_{1g}(F)\rightarrow{}^4A_{2g}(F)$ (ν_2) and $^4T_{1g}(F)\rightarrow{}^4T_{2g}(P)$ (ν_3) transitions, respectively[28]. Due to the instrument's narrow range, it was impossible to witness the lowest band, ν_1, but Underhill and Billing's suggested[29] band fitting method allowed for its calculation. In an octahedral environment, the Ni (II) complex exhibited two absorption bands at 660 and 415nm, which correspond to $^3A_{2g}(F)\rightarrow{}^3T_1g(F)$ (ν_2) and $^3A_{2g}(F)\rightarrow{}^3T_{1g}(P)$ (ν_3) transitions, respectively. A band fitting procedure was used[29] to calculate band ν_1.

Magnetic moment measurements reveal that the Pd (II) complex is diamagnetic with a spin-paired d^8 system. Three *d-d* bands are observed at 565, 503, and 451 nm, which could be assigned to o $^1A_{1g}\rightarrow{}^1A_2g$, $^1A_{1g}\rightarrow{}^1B_{1g}$, and $^1A_{1g}\rightarrow{}^1E_g$ transitions. This complex's electronic spectrum indicates square-planar geometry around the palladium (II) ion[30]. The Cu (II) complex, which is light green in hue, showed a single broad asymmetric band between 710 and 620 nm. The three transitions $^2B_{1g}\rightarrow{}^2A_{1g}$ (ν_1), $^2B_{1g}\rightarrow{}^2B_{2g}$ (ν_2), and $^2B_{1g}\rightarrow{}^2E_g$ (ν_3), which are of identical energy and give birth to only one broad absorption band, are indicated by the band's broadness. The band's width may be caused by Jahn-Teller distortion in motion. This information revealed a deformed octahedral geometry surrounding the Cu (II) ion[31]. Weak absorption bands at 537nm (ν_1), 422nm (ν_2), 360nm (ν_3), and 257nm (ν_4), which are indicative of octahedral geometry and correspond to the transitions $^6A_{1g}\rightarrow{}^4T_{1g}(^4G)$, $^6A_{1g}\rightarrow{}^4E_g(^4D)$, $^6A_{1g}\rightarrow{}^4T_{1g}(^4P)$ and $^6A_{1g}\rightarrow{}^4E_g(G)$, respectively. The complex displays a magnetic moment in the 5.90 B.M. range[32]. Bands at 474 and 512 nm are observed in the electronic spectra of the complexes for Zn (II), whereas bands at 550 and 534 nm are visible for Cd (II) and Hg (II), respectively. Metal-to-ligand charge transfer could be the cause of these bands[33].

Table-3: UV-Visible spectral data of HDMH*m*HB ligand and its Transition metal (II) complexes

Compound	λnm	ε (dm³/mol/cm)	Transition
HDMH*m*HB	366	12664	$\pi^* \leftarrow \pi$
	298	7980	$\pi^* \leftarrow \pi$
	255	7198	$\pi^* \leftarrow \pi$
[Fe(DMH*m*HB)₂]	905	3	$^5T_{2g} \leftarrow {}^5E_g$
[Co(DMH*m*HB)₂]	678	721	$^4T_{1g}(F) \rightarrow {}^4A_{2g}(F)$ (ν_2)
	608	814	$^4T_{1g}(F) \rightarrow {}^4T_{2g}(P)$ (ν_3)
[Ni(DMH*m*HB)₂]	660	596	$^3A_{2g}(F) \rightarrow {}^3T_1g(F)$ (ν_2)
	415	5499	$^3A_{2g}(F) \rightarrow {}^3T_{1g}(P)$
[Pd(DMH*m*HB)₂]	565	347	$^1A_{1g} \rightarrow {}^1A_2g$
	503	587	$^1A_{1g} \rightarrow {}^1B_{1g}$
	451	1058	$^1A_{1g} \rightarrow {}^1E_g$
[Cu(DMH*m*HB)₂]	710	319	$^2B_{1g} \rightarrow {}^2A_{1g}(\nu_1)$
	653	536	$^2B_{1g} \rightarrow {}^2B_{2g}$ (ν_2)
	620	947	$^2B_{1g} \rightarrow {}^2E_g$ (ν_3)
[Mn(DMH*m*HB)₂]	537	356	$^6A_{1g} \rightarrow {}^4T_{1g}(^4G)$
	422	963	$^6A_{1g} \rightarrow {}^4E_g(^4D)$
	360	1056	$^6A_{1g} \rightarrow {}^4T_{1g}(^4P)$
	257	3547	$^6A_{1g} \rightarrow {}^4E_g(G)$
[Zn(DMH*m*HB)₂]	512	1530	MLCT
	474	2458	MLCT
[Cd(DMH*m*HB)₂]	550	2670	MLCT
[Hg(DMH*m*HB)₂]	534	3567	MLCT

3.3. PMR spectra:

The ^{1}H NMR (400 MHz and δ/ppm) in DMSO-d6 characterised the synthesised ligands. All the spectra agree with the proposed structure of the ligand. The ^{1}H NMR spectrum of the synthesised ligand showed distinguished NMR signals. The ^{1}H NMR spectrum of the prepared ligand show singlet due to oximino –OH proton at 11.52 ppm. In prepared diamagnetic metal complexes, this band disappeared, indicating that oximino group participated in complexation via deprotonation. The characteristic proton of phenol appeared at 11.26 ppm. The signal of CH is found at 9.00 ppm. Aromatic protons found in the 6.81-7.19 ppm range are assigned to aromatic protons.

Table-4: PMR spectrum of HDMH*m*HB and its Transition metal (II) complexes in d_6 DMSO

Compound	Oximino –OH	Phenolic -OH	-CH=	Phenyl Ring	-CH₃
HDMH*m*HB	11.52	11.26	9.00	6.81-7.19	2.51
[Pd(DMH*m*HB)₂]	-	11.19	9.02	7.00-7.40	2.52
[Zn(DMH*m*HB)₂]	-	11.20	9.00	6.81-7.19	2.50
[Cd(DMH*m*HB)₂]	-	11.25	9.03	7.01-7.38	2.49
[Hg(DMH*m*HB)₂]	-	11.19	9.00	7.08-7.42	2.53

3.4. ESR Spectra:

ESR spectra ESR spectrum of the Cu (II) complex is recorded at LNT. The lack of Cu-Cu interactions can be explained by proposing transitions, i.e. Ms = 2 between two paramagnetic centres[34]. The spectra analysis yielded $g_{||}$ = 2.2301 and $g_{\perp}$ = 2.078. The values $g_{||} > g_{\perp}$ indicate that the unpaired electron is in the d_{x2-y2} orbital, resulting in the ground state $^2B_{1g}$. This supports the notion that there is a significant mixing of ground and excited state terms, which is also reflected in magnetic moment values slightly greater than the spin-only value for Cu(II), i.e. 1.93BM, indicating the formation of mononuclear copper(II) complexes[35]. The ratio $g_{||} > g_{\perp} > g_{ave} > 2.0023$ evaluated for all Cu(II) complexes, suggesting that the unpaired electron is localised in d_{x2-y2} orbital and the spectral features are characteristic of tetragonally distorted octahedron[36-37].

Biological Studies

Antibacterial studies

Zones of inhibition against S. aureus, B. subtilis, E. coli, and P. aeruginosa ranged from 16.9 mm to 30.5 mm in the antibacterial screening results. In addition, the metal complexes were more effective than the HDMH*m*HB ligand against Staphylococcus aureus, with inhibitory values ranging from 6 to 7 mm. An increase in lipophilic character that permits penetration into the lipid

layers of the bacterial membrane can be traced back to the chelation theory effect, which reduces the polarity of the metal atom by partially exchanging its charge with donor groups of the ligand. The inhibitory zone value of the Ni (II) complex against Escherichia coli was 19 mm, the highest of any compounds or even the reference drugs *streptomycin*, which had a value of 12 mm. The coordination of Hg^{2+} metal with the ligands makes Hg(II) complex more bioactive and hazardous, allowing it to easily penetrate the cell-lipid barrier and impede and destroy the test organism's respiration process, accounting for the complex's more significant value. Inhibitory zone measurements for S. aureus, B. subtilis, E. coli, and P. aeruginosa were 12 mm, 11 mm, 16 mm, and 13 mm for the Hg(II) complex, respectively; for streptomycin, these measurements were 10 mm, 10 mm, 12 mm, and 14 mm. It has been reported that test compounds can be more effective against bacteria than the standard streptomycin.

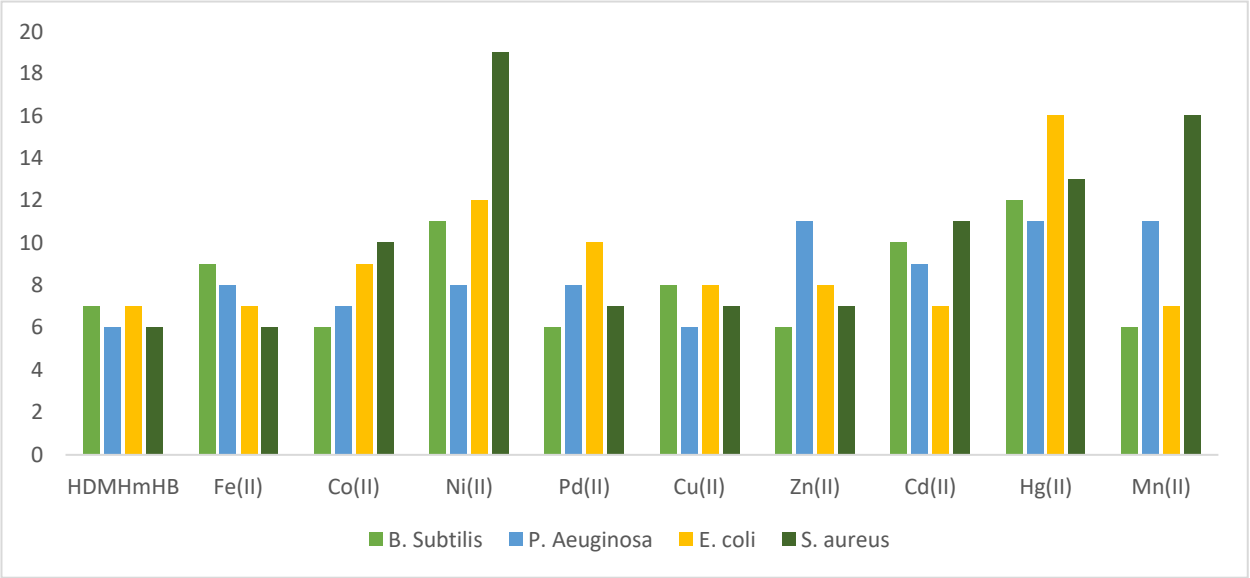

Figure 3: Bar graph of antibacterial activities of prepared compounds in mm

Antifungal studies

The ligand and its complexes had about two and a half times the potency (12-22 mm) compared to fluconazole (11-16 mm), except for the Mn(II) complex, whose (6 mm) zone of inhibition against C Albicans was very close to fluconazole (11 mm). C Albican and S. C. failed to dissolve transition compounds.

4. Conclusion:

The novel ligand was developed by mixing diacetylmonoximehydrazide and 3-hydroxybenzaldehyde. Reactions of Fe^{II}, Mn^{II}, Co^{II}, Ni^{II}, Pd^{II}, Cu^{II}, Zn^{II}, Hg^{II}, and Cd^{II} metal salts developed coloured complexes. Elemental analysis, physicochemical studies, FT(IR), ^1H NMR, UV-Vis, ESR measurements, magnetic susceptibility, and molar conductivity measurements were used to define the synthesised compounds. The complexes may be proposed to have square planar geometry for Pd(II) complex, tetrahedral geometry for Zn^{II}, Hg^{II}, and Cd^{II} complexes and octahedral geometry around Fe^{II}, Mn^{II}, Co^{II}, Ni^{II}, and Cu^{II} complexes based on the physicochemical and spectroscopic results presented above. It was observed that every metal compound that had been synthesised was mononuclear.

5. References:

1. Pilichos, E., Mylonas-Margaritis, I., Kontos, A. P., Psycharis, V., Klouras, N., Raptopoulou, C. P., & Perlepes, S. P. (2018). Coordination and metal ion-mediated transformation of a polydentate ligand containing oxime, hydrazone and picolinate functionalities. Inorganic Chemistry Communications, 94, 48–52. doi:10.1016/j.inoche.2018.06.004.
2. El-Saied, F. A., Salem, T. A., Shakdofa, M. M. E., Al-Hakimi, A. N., & Radwan, A. S. (2017). Antitumor activity of synthesised and characterised Cu(II), Ni(II) and Co(II) complexes of hydrazone-oxime ligands derived from 3-(hydroxyimino) butan-2-one. Beni-Suef University Journal of Basic and Applied Sciences. doi:10.1016/j.bjbas.2017.09.002.
3. Shakdofa, M. M. E., Morsy, N. A., Rasras, A. J., Al-Hakimi, A. N., & Shakdofa, A. M. E. (2020). Synthesis, characterization, and density functional theory studies of hydrazone–oxime

ligand derived from 2,4,6-trichlorophenyl hydrazine and its metal complexes searching for new antimicrobial drugs. Applied Organometallic Chemistry, 35(2). doi:10.1002/aoc.6111.

4. Shakdofa, M. M. E., El-Saied, F. A., Rasras, A. J., & Al-Hakimi, A. N. (2018). Transition metal complexes of a hydrazone-oxime ligand containing the isonicotinoyl moiety: Synthesis, characterization and microbicide activities. Applied Organometallic Chemistry, 32(7), e4376. doi:10.1002/aoc.4376.
5. Nasrallah, D. J., Zehnder, T. E., Ludwig, J. R., Steigerwald, D. C., Kiernicki, J. J., Szymczak, N. K., & Schindler, C. S. (2022). Hydrazone and Oxime Olefination via Ruthenium Alkylidenes. Angewandte Chemie International Edition, 61(22), e202112101.
6. Kölmel, D. K., & Kool, E. T. (2017). Oximes and Hydrazones in Bioconjugation: Mechanism and Catalysis. Chemical Reviews, 117(15), 10358–10376. doi:10.1021/acs.chemrev.7b00090.
7. Stress, C. J., Schmidt, P. J., & Gillingham, D. G. (2016). Comparison of boron-assisted oxime and hydrazone formations leads to the discovery of a fluorogenic variant. Organic & Biomolecular Chemistry, 14(24), 5529–5533. doi:10.1039/c6ob00168h.
8. Hania, M. M. (2009). Synthesis and Antibacterial Activity of Some Transition Metal Complexes of Oxime, Semicarbazone and Phenylhydrazone. E-Journal of Chemistry, 6(s1), S508–S514. doi:10.1155/2009/204714.
9. El-Metwally, N. M., & El-Asmy, A. A. (2006). Chelating activity of bis (diacetylmonoxime) thiocarbohydrazone towards VO2+, Co(II), Ni(II), Cu(II) and Pt(IV) ions. Journal of Coordination Chemistry, 59(14), 1591–1601. doi:10.1080/00958970600572743.
10. Babahan, I., Özmen, A., Aksel, M., Bilgin, M. D., Gumusada, R., Gunay, M. E., & Eyduran, F. (2020). A novel bidentate ligand containing oxime, hydrazone and indole moieties and its BF2 + bridged transition metal complexes and their efficiency against prostate and breast cancer cells. Applied Organometallic Chemistry, e5632. doi:10.1002/aoc.5632.
11. Naskar, S., Naskar, S., Mondal, S., Majhi, P. K., Drew, M. G. B., & Chattopadhyay, S. K. (2011). Synthesis and spectroscopic properties of cobalt(III) complexes of some aroyl hydrazones: X-ray crystal structures of one cobalt(III) complex and two aroyl hydrazone ligands. Inorganica Chimica Acta, 371(1), 100–106. doi:10.1016/j.ica.2011.03.051.
12. Khedr, A. M., Gaber, M., & Diab, H. A. (2012). Synthesis, characterization, molecular modeling, and thermal analyses of bioactive Co(II) and Cu(II) complexes with diacetylmonoxime and different amines. Journal of Coordination Chemistry, 65(10), 1672–1684. doi:10.1080/00958972.2012.678338.
13. El-Hendawy, A. M., Fayed, A. M., & Mostafa, M. R. (2011). Complexes of a diacetylmonoxime Schiff base of S-methyldithiocarbazate (H2damsm) with Fe(III), Ru(III)/Ru(II), and V(IV); catalytic activity and X-ray crystal structure of [Fe(Hdamsm) 2]NO3·H2O. Transition Metal Chemistry, 36(4), 351–361. doi:10.1007/s11243-011-9477-z.
14. Salem, N. M. H., El-Sayed, L., & Iskander, M. F. (2008). Metal complexes derived from hydrazoneoxime ligands: IV. Molecular and supramolecular structures of some nickel(II) complexes derived from diacetylmonoxime S-benzyldithiocarbazonate. Polyhedron, 27(15), 3215–3226. doi:10.1016/j.poly.2008.07.009.
15. R. Yaul, A., V. Dhande, V., B. Pethe, G., & S. Aswar, A. (2014). Synthesis, characterization, biological and electrical conductivity studies of some Schiff base metal complexes. Bulletin of the Chemical Society of Ethiopia, 28(2), 255. doi:10.4314/bcse.v28i2.9.
16. Pu, Y., Dong, Z., Zhang, P., Wu, Y., Zhao, J., & Luo, Y. (2016). Dielectric, complex impedance and electrical conductivity studies of the multiferroic Sr 2 FeSi 2 O 7 -crystallized glass-ceramics. Journal of Alloys and Compounds, 672, 64–71. doi:10.1016/j.jallcom.2016.02.137.
17. Smith, A. (2003). The structures of phenolic oximes and their complexes. Coordination Chemistry Reviews, 241(1-2), 61–85. doi:10.1016/s0010-8545(02)00310-7.
18. Bajju, G. D., Kundan, S., Bhagat, M., Gupta, D., Kapahi, A., & Devi, G. (2014). Synthesis and Spectroscopic and Biological Activities of Zn(II) Porphyrin with Oxygen Donors. Bioinorganic Chemistry and Applications, 2014, 1–13. doi:10.1155/2014/782762.
19. Ozkan, G., Kose, M., Zengin, H., McKee, V., & Kurtoglu, M. (2015). A new Salen-type azo–azomethine ligand and its Ni(II), Cu(II) and Zn(II) complexes: Synthesis, spectral characterization, crystal structure and photoluminescence studies. Spectrochimica Acta Part A: Molecular and Biomolecular Spectroscopy, 150, 966–973.

doi:10.1016/j.saa.2015.06.038.

20. Yeğiner, G., Gülcan, M., Işık, S., Ürüt, G. Ö., Özdemir, S., & Kurtoğlu, M. (2017). Transition Metal (II) Complexes with a Novel Azo-azomethine Schiff Base Ligand: Synthesis, Structural and Spectroscopic Characterization, Thermal Properties and Biological Applications. Journal of Fluorescence, 27(6), 2239–2251. doi:10.1007/s10895-017-2166-3.
21. Sahan, F., Kose, M., Hepokur, C., Karakas, D., & Kurtoglu, M. (2019). New azo-azomethine-based transition metal complexes: Synthesis, spectroscopy, solid-state structure, density functional theory calculations and anticancer studies. Applied Organometallic Chemistry, e4954. doi:10.1002/aoc.4954.
22. Kaya, Y., Irez, G., Mutlu, H., & Buyukgungor, O. (2011). A Novel Reaction of α-Carbonyl Oxime and Amido Alcohol: Synthesis, Characterization, Crystal Structure, and Thermal Studies of an Amido Alcohol, a New Oximino Alcohol Ligand, and its Metal Complexes. Synthesis and Reactivity in Inorganic, Metal-Organic, and Nano-Metal Chemistry, 41(7), 754–762. doi:10.1080/15533174.2011.591300.
23. Choi, S., Ha, S., & Park, C.-M. (2017). α-Diazo oxime ethers for N-heterocycle synthesis. Chemical Communications, 53(45), 6054–6064. doi:10.1039/c7cc02650a.
24. Opalade, A. A., Gomez-Garcia, C. J., & Gerasimchuk, N. (2019). New Route to Polynuclear Ni(II) and Cu(II) Complexes with Bridging Oxime Groups which are Inaccessible by Conventional Preparations. Crystal Growth & Design. doi:10.1021/acs.cgd.8b01262.
25. Jetley, U. K., Singh, B. K., Garg, B. S., & Mishra, P. (2007). Synthesis, characterization and XRPD studies of the bioactive complex of 2-hydroxy-3,5-dimethyl acetophenoneoxime (HDMAOX) with oxovanadium(IV). Journal of Coordination Chemistry, 60(20), 2243–2255. doi:10.1080/00958970701260305.
26. Semakin, A. N., Sukhorukov, A. Y., Lesiv, A. V., Ioffe, S. L., Lyssenko, K. A., Nelyubina, Y. V., & Tartakovsky, V. A. (2009). Unusual Intramolecular Cyclization of Tris(β-oximinoalkyl)amines. The First Synthesis of 1,4,6,10-Tetraazaadamantanes. Organic Letters, 11(18), 4072–4075. doi:10.1021/ol9015157.
27. Daniel, V. P., Murukan, B., Kumari, B. S., & Mohanan, K. (2008). Synthesis, spectroscopic characterization, electrochemical behaviour, reactivity and antibacterial activity of some transition metal complexes with 2-(N-salicylideneamino)-3-carboxyethyl-4,5-dimethylthiophene. Spectrochimica Acta Part A: Molecular and Biomolecular Spectroscopy, 70(2), 403–410. doi:10.1016/j.saa.2007.11.003.
28. Angelusiu, M. V., Barbuceanu, S.-F., Draghici, C., & Almajan, G. L. (2010). New Cu(II), Co(II), Ni(II) complexes with aroyl-hydrazone based ligand. Synthesis, spectroscopic characterization and in vitro antibacterial evaluation. European Journal of Medicinal Chemistry, 45(5), 2055–2062. doi:10.1016/j.ejmech.2010.01.033.
29. Underhill, A. E., & Billing, D. E. (1966). Calculations of the Racah Parameter B for Nickel (II) and Cobalt (II) Compounds. Nature, 210(5038), 834–835. doi:10.1038/210834a0.
30. Sayin, K., Kariper, S. E., Taştan, M., Sayin, T. A., & Karakaş, D. (2018). Investigations of structural, spectral, electronic and biological properties of N-heterocyclic carbene Ag(I) and Pd(II) complexes. Journal of Molecular Structure. doi:10.1016/j.molstruc.2018.08.103.
31. Abdel-Rahman, L. H., Abu-Dief, A. M., Moustafa, H., & Hamdan, S. K. (2016). Ni(II) and Cu(II) complexes with ONNO asymmetric tetradentate Schiff base ligand: synthesis, spectroscopic characterization, theoretical calculations, DNA interaction and antimicrobial studies. Applied Organometallic Chemistry, 31(2), e3555. doi:10.1002/aoc.3555.
32. Chandra, S., & Kumar, U. (2005). Spectral and magnetic studies on manganese(II), cobalt(II) and nickel(II) complexes with Schiff bases. Spectrochimica Acta Part A: Molecular and Biomolecular Spectroscopy, 61(1-2), 219–224. doi:10.1016/j.saa.2004.03.036.
33. El-Gammal, O. A., Rakha, T. H., Metwally, H. M., & Abu El-Reash, G. M. (2014). Synthesis, characterization, DFT and biological studies of isatinpicolinohydrazone and its Zn(II), Cd(II) and Hg(II) complexes. Spectrochimica Acta Part A: Molecular and Biomolecular Spectroscopy, 127, 144–156. doi:10.1016/j.saa.2014.02.008.
34. Singh, V. P. (2008). Synthesis, electronic and ESR spectral studies on copper(II) nitrate complexes with some acylhydrazines and hydrazones. Spectrochimica Acta Part A: Molecular and Biomolecular Spectroscopy, 71(1), 17–22. doi:10.1016/j.saa.2007.11.004.
35. Patel, R. N., Singh, N., Shukla, K. K., & Gundla, V. L. N. (2005). E.S.R., magnetic, electronic and superoxide dismutase studies of imidazolate-bridged Cu(II)–Cu(II) complexes with ethylenediamine as capping ligand. Spectrochimica Acta Part A: Molecular and

Biomolecular Spectroscopy, 61(8), 1893–1897. doi:10.1016/j.saa.2004.07.019.

36. Chandra, S., Gautam, A., & Tyagi, M. (2009). Synthesis, structural characterization, and antibacterial studies of a tetradentate macrocyclic ligand and Its Co(II), Ni(II), and Cu(II) complexes. Russian Journal of Coordination Chemistry, 35(1), 25–29. doi:10.1134/s1070328409010060.
37. El-Sonbati, A. Z., Diab, M. A., El-Bindary, A. A., & Nozha, S. G. (2011). Structural and characterization of novel copper(II) azodye complexes. Spectrochimica Acta Part A: Molecular and Biomolecular Spectroscopy, 83(1), 490–498. doi:10.1016/j.saa.2011.08.070.